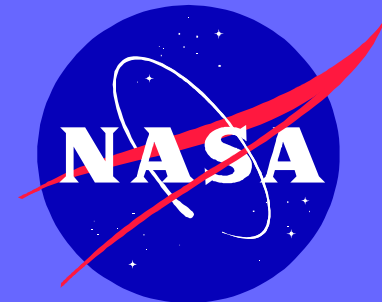
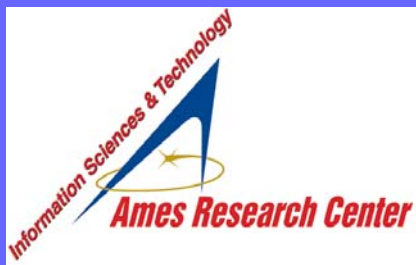


Automatic Balancing and Intelligent Fault Tolerance for a Space-Based Centrifuge

Edward Wilson
Intellization, Redwood Shores, CA
Ed.Wilson@intellization.com

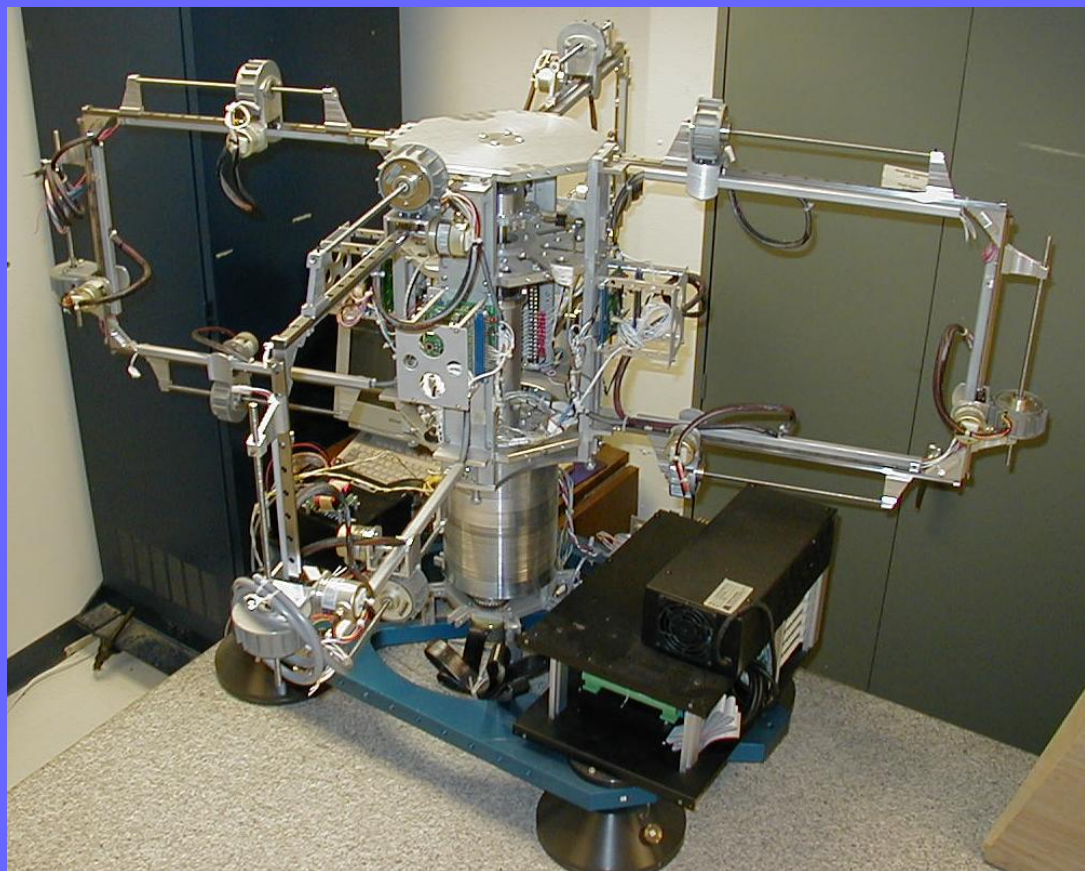
Robert W. Mah
NASA Ames Research Center, Moffett Field, CA
Robert.W.Mah@nasa.gov



Research objective: Develop automatic balancing system for a space-based centrifuge, providing fault tolerance using existing sensors and actuators (a software-only solution). Develop and validate through application on realistic simulations and hardware.

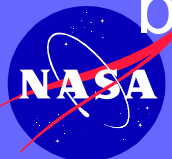
Outline:

- Introduction
- Imbalance ID, balancing
- Maximum-likelihood FDI, reconfiguration
- MATLAB Demo

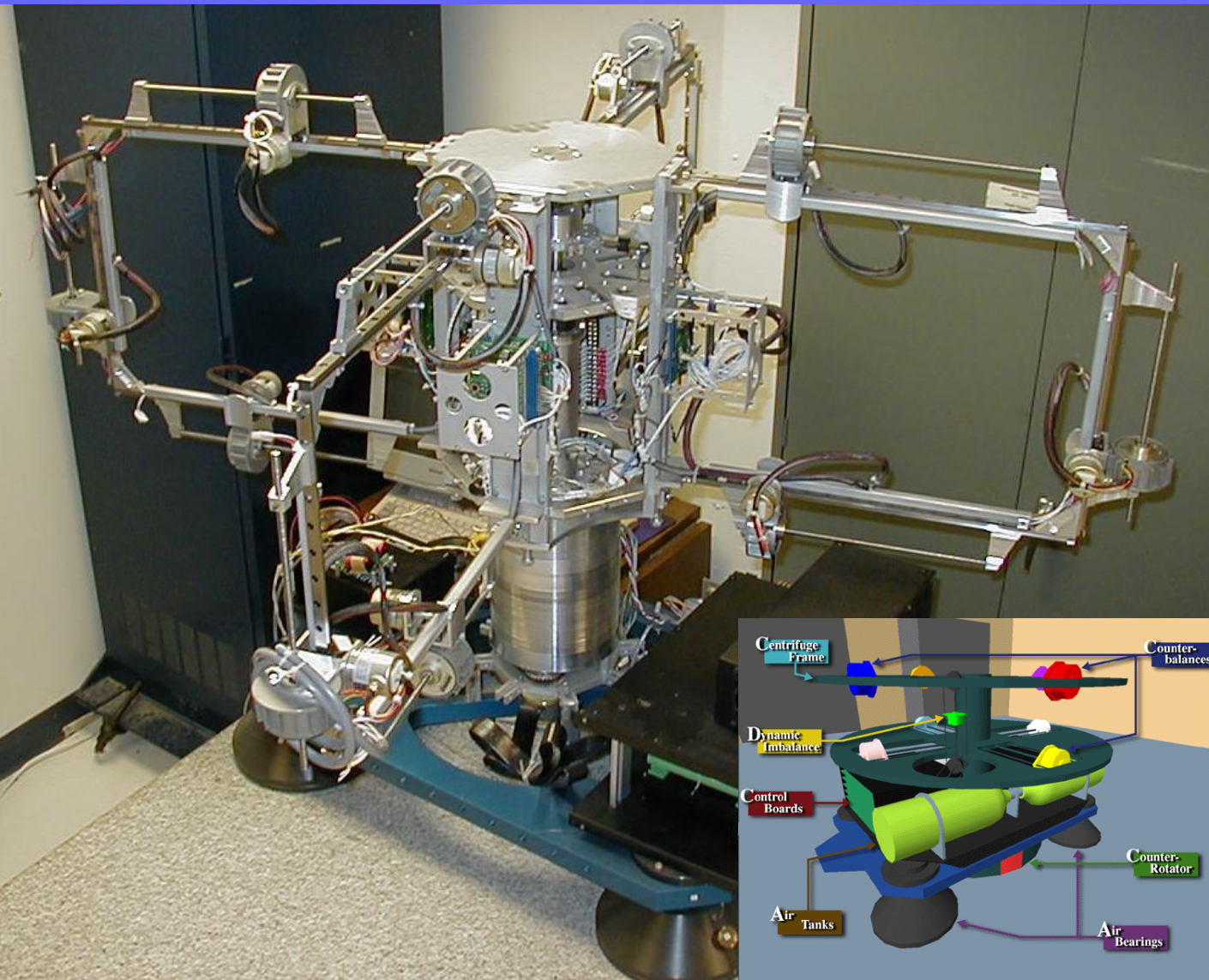


Introduction

- Space-based centrifuge—biological experiments, Mars (0.38g), Moon (0.16g), Control
- ISS Centrifuge: JAXA led, 2.5 m diameter, 0.1-2.0g, 2 ton rotor, 5-axis suspension
- Strict vibration requirements for other micro-g experiments on ISS → automatic balancing/vibration isolation systems required
- Ames SSRL centrifuge: 1993-1995, fixed spin axis, strain gauges, hardware prototype, research focused on autobalancing and FDIR
- The identification, balancing, and FDIR methods are extensible to the ISS centrifuge configuration as a software update. Also relevant to other ID / balancing / FDIR applications.



NASA Ames SSRL Centrifuge



Built 1993-1995

12 CWs

Fixed and spinning

Strain gauges

Fixed spin axis

Air bearings

0-g vs. 1-g testing

→ MSC ADAMS

Diff vs. ISS Cent:

fixed spin axis

vs. VIM

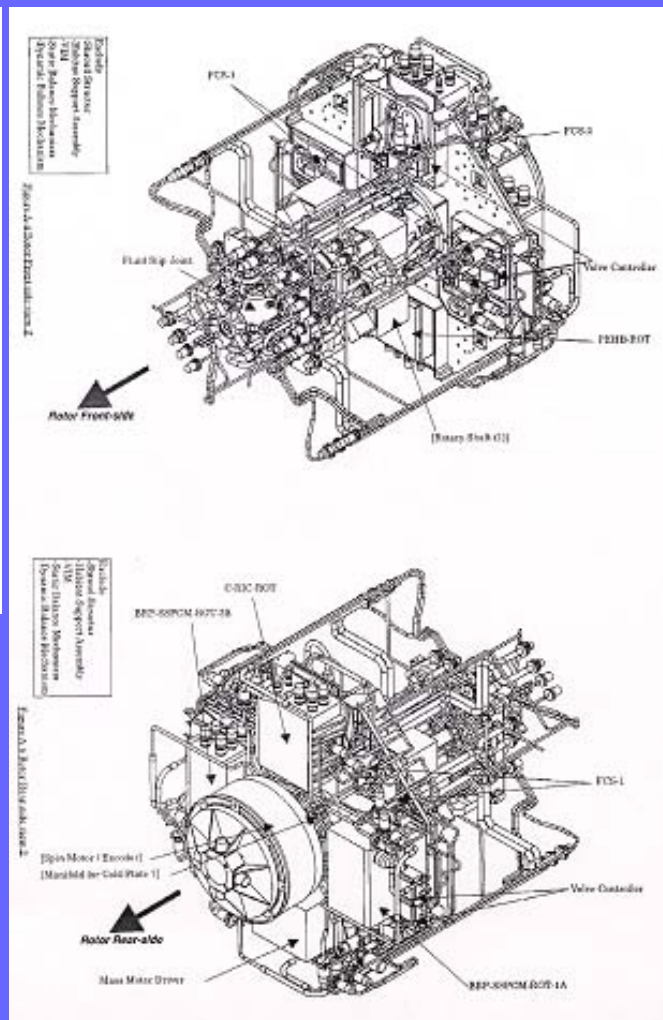
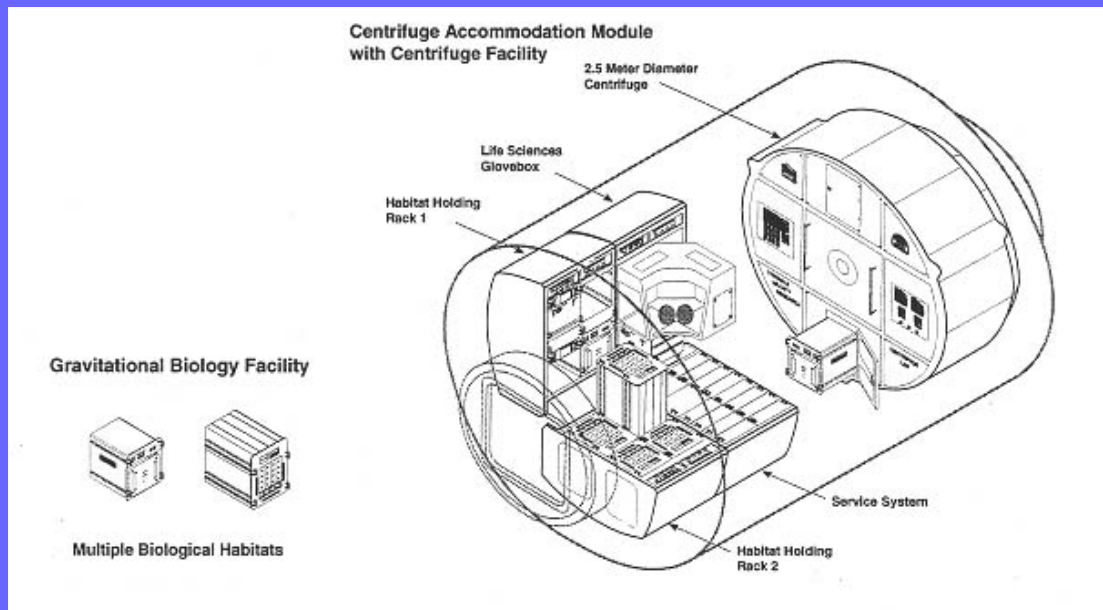
SG vs. BDS

CW configuration

However, key
concepts extend to
ISS



International Space Station artificial gravity centrifuge

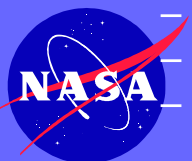


- Otsuki, F., Uematsu, H., Nakamura, Y., Ohtomi, K., Chida, Y., Kawamoto, O., "Approach to Realization of Micro-gravity Performance of Centrifuge Rotor System," Copyright 1998 Society of Automotive Engineers, Inc.
- Otsuki, F., Uematsu, H., Nakamura, Y., Chida, Y., Nishimura, O., Ohtomi, K., and Tanaka, M., "Vibration Isolation Control of Centrifuge Rotor," *5th International Conference on Motion and Vibration Control*, 2000, pp. 415-420.
- Ohtomi, K., Otsuki, F., Uematsu, H., Nakamura, Y., Chida, Y., and Kawamoto, O., "Approach to Realization of Micro-gravity Performance of Centrifuge Rotor," *30th International Conference on Environmental Systems Proceedings*, 2000.
- Ohtomi, K., Otsuki, F., Uematsu, H., Nakamura, Y., Chida, Y., Nishimura, O., and Okamura, R., "Active Mass Auto-balancing System for Centrifuge Rotor Providing an Artificial Gravity in Space," *31st International Conference on Environmental Systems Proceedings*, 2001.
- Ohtomi, K., "Centrifuge rotor integrated analysis," *Modeling, Simulation and Calibration of Space-based Systems*, SPIE Vol. 5420, April 2004.

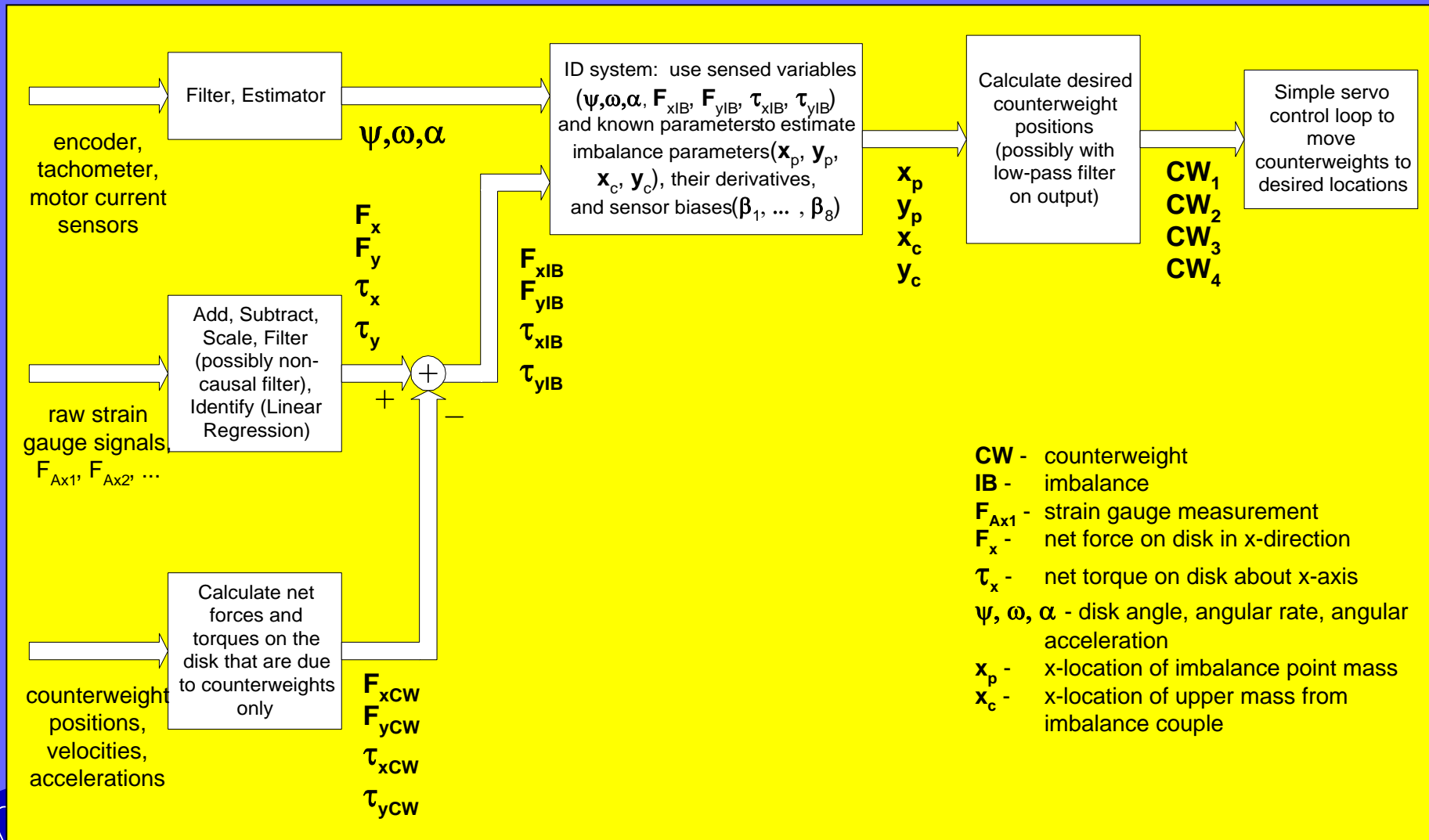


Autobalancing algorithm summary

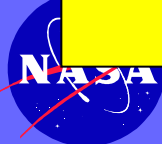
- 2-step, indirect method: (1) ID imbalance, then (2) null with counterweights (CWs)
- Architecture similar to indirect adaptive control
- Rotor modeled as rigid body spinning about fixed axis
- Rotor imbalance represented in a compact, intuitive way: x- and y-locations of a point mass in a central plane and pair of asymmetrically located point masses in off-central planes. This four-parameter representation is sufficient to represent an arbitrary imbalance and can be intuitively related to counterweight motions.
- Step 1. Rotor imbalance (not including counterweights) estimated at each sample period:
 - 1a. Sensor signals (strain gauges, counterweight positions, velocities, and accelerations, rotor angle encoder and tachometer) are combined, using a least-squares fit, to calculate the estimated net rotor force and torque in x and y created by the imbalance (4 variables).
 - 1b. The four imbalance parameters (and possibly their derivatives) are estimated using these forces and torques. This uses a dynamic model of the rotor that calculates effects due to the position, velocity, and acceleration of the imbalance parameters.
- Step 2. CWs are driven to exactly counteract the estimated rotor imbalance.
- In a direct method, sensor signals are used (filtered, and mathematically manipulated) to directly drive the counterweights. Increased complexity of indirect method enables more accurate fitting of the sensor data to the rotor imbalance dynamical model. Performance / complexity tradeoff depends on noise, imbalance characteristics (how fast it is moving, etc.), model uncertainty.
- This indirect, segmented method has other benefits:
 - Facilitates sensor and CW FDIR
 - Facilitates redesign to accommodate hardware design changes
 - Robust to unknown or uncertain dynamics
 - Enables independent tuning of ID vs. CW motion control



Control system architecture

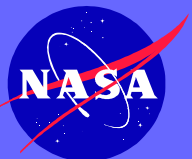


- CW** - counterweight
- IB** - imbalance
- F_{Ax1} - strain gauge measurement
- F_x - net force on disk in x-direction
- τ_x - net torque on disk about x-axis
- ψ, ω, α - disk angle, angular rate, angular acceleration
- x_p - x-location of imbalance point mass
- x_c - x-location of upper mass from imbalance couple



Initial combination of rotor sensor signals – helps ID and FDIR

- All sensors (SGs, CWs, velocities, and accelerations, rotor angle encoder and tachometer) are used at each sample to estimate four variables: net rotor force and torque in x and y.
- Done by least squares (LS) fit to the data, using model of sensor geometry and subtracting out known CW forces.
- These four variables then pass to imbalance ID algorithm.
- Benefits of segmenting the ID into these two parts:
 - Physically, the four imbalance parameters are directly related to these four intermediate variables. Relation between sensor values and these intermediate variables is more direct than that between sensor values and imbalance parameters. This logically separates estimation of forces and torques created by the imbalance from the estimation of imbalance parameters themselves.
 - Facilitates sensor FDIR, since analysis can be performed without regard to imbalance dynamics—can analyze residuals in the estimation of the intermediate variables.
 - If sensors change (failure, design change, etc.), second part of ID (that finds imbalance parameters from estimated forces and torques) does not change.
 - Overall complexity is reduced by breaking one large problem into two smaller ones. No accuracy is lost, due to the physical reasoning listed in the first bullet.



LS estimation of rotor net force and torque at each sample

$$S = \begin{bmatrix} S_{Axf} \\ S_{Ayf} \\ S_{Bxf} \\ S_{Byf} \\ S_{Axs} \\ S_{Ays} \\ S_{Bxs} \\ S_{Bys} \end{bmatrix}; S_{true} = \begin{bmatrix} S_{Axf_{true}} \\ S_{Ayf_{true}} \\ S_{Bxf_{true}} \\ S_{Byf_{true}} \\ S_{Axs_{true}} \\ S_{Ays_{true}} \\ S_{Bxs_{true}} \\ S_{Bys_{true}} \end{bmatrix}; B = \begin{bmatrix} \beta_1 \\ \beta_2 \\ \beta_3 \\ \beta_4 \\ \beta_5 \\ \beta_6 \\ \beta_7 \\ \beta_8 \end{bmatrix}; E_{SSN} = \begin{bmatrix} \epsilon_{SSN1} \\ \epsilon_{SSN2} \\ \epsilon_{SSN3} \\ \epsilon_{SSN4} \\ \epsilon_{SSN5} \\ \epsilon_{SSN6} \\ \epsilon_{SSN7} \\ \epsilon_{SSN8} \end{bmatrix}$$

$$S_{true} = TGF_{net} + E_{SFN}$$

$$S = TGF_{net} + B + E_{SFN} + E_{SSN}$$

$$F_{net} = [F_x \quad F_y \quad \tau_x \quad \tau_y]^T$$

$$\hat{F}_{net} = \left((G^T G)^{-1} G^T \right) (T^{-1} (S - B))$$

$$\hat{F}_{net} = \Gamma T^{-1} (S - B)$$

$$T = \begin{bmatrix} c\psi & -s\psi & 0 & 0 & 0 & 0 & 0 & 0 \\ s\psi & c\psi & 0 & 0 & 0 & 0 & 0 & 0 \\ 0 & 0 & c\psi & -s\psi & 0 & 0 & 0 & 0 \\ 0 & 0 & s\psi & c\psi & 0 & 0 & 0 & 0 \\ 0 & 0 & 0 & 0 & 1 & 0 & 0 & 0 \\ 0 & 0 & 0 & 0 & 0 & 1 & 0 & 0 \\ 0 & 0 & 0 & 0 & 0 & 0 & 1 & 0 \\ 0 & 0 & 0 & 0 & 0 & 0 & 0 & 1 \end{bmatrix}$$

$$G = \begin{bmatrix} \frac{-z_{Bf}}{z_{Af} - z_{Bf}} & 0 & 0 & \frac{1}{z_{Af} - z_{Bf}} \\ 0 & \frac{-z_{Bf}}{z_{Af} - z_{Bf}} & \frac{-1}{z_{Af} - z_{Bf}} & 0 \\ \frac{z_{Af}}{z_{Af} - z_{Bf}} & 0 & 0 & \frac{-1}{z_{Af} - z_{Bf}} \\ 0 & \frac{z_{Af}}{z_{Af} - z_{Bf}} & \frac{1}{z_{Af} - z_{Bf}} & 0 \\ \frac{-z_{Bs}}{z_{As} - z_{Bs}} & 0 & 0 & \frac{1}{z_{As} - z_{Bs}} \\ 0 & \frac{-z_{Bs}}{z_{As} - z_{Bs}} & \frac{-1}{z_{As} - z_{Bs}} & 0 \\ \frac{z_{As}}{z_{As} - z_{Bs}} & 0 & 0 & \frac{-1}{z_{As} - z_{Bs}} \\ 0 & \frac{z_{As}}{z_{As} - z_{Bs}} & \frac{1}{z_{As} - z_{Bs}} & 0 \end{bmatrix}$$

$$T^{-1} = \begin{bmatrix} c\psi & s\psi & 0 & 0 & 0 & 0 & 0 & 0 \\ -s\psi & c\psi & 0 & 0 & 0 & 0 & 0 & 0 \\ 0 & 0 & c\psi & s\psi & 0 & 0 & 0 & 0 \\ 0 & 0 & -s\psi & c\psi & 0 & 0 & 0 & 0 \\ 0 & 0 & 0 & 0 & 1 & 0 & 0 & 0 \\ 0 & 0 & 0 & 0 & 0 & 1 & 0 & 0 \\ 0 & 0 & 0 & 0 & 0 & 0 & 1 & 0 \\ 0 & 0 & 0 & 0 & 0 & 0 & 0 & 1 \end{bmatrix}, S \square \begin{bmatrix} S_{Axf} \\ S_{Ayf} \\ S_{Bxf} \\ S_{Byf} \\ S_{Axs} \\ S_{Ays} \\ S_{Bxs} \\ S_{Bys} \end{bmatrix}, B \square \begin{bmatrix} \beta_1 \\ \beta_2 \\ \beta_3 \\ \beta_4 \\ \beta_5 \\ \beta_6 \\ \beta_7 \\ \beta_8 \end{bmatrix}$$

$$\Gamma \square (G^T G)^{-1} G^T = \begin{bmatrix} \Gamma_{11} & 0 & \Gamma_{13} & 0 & \Gamma_{15} & 0 & \Gamma_{17} & 0 \\ 0 & \Gamma_{11} & 0 & \Gamma_{13} & 0 & \Gamma_{15} & 0 & \Gamma_{17} \\ 0 & \Gamma_{32} & 0 & \Gamma_{34} & 0 & \Gamma_{36} & 0 & \Gamma_{38} \\ -\Gamma_{32} & 0 & -\Gamma_{34} & 0 & -\Gamma_{36} & 0 & -\Gamma_{38} & 0 \end{bmatrix}$$

Sensor FDIR

FDI approach taken here is based upon maximum likelihood theory. Loosely analogous to the commonly applied bank of Kalman filters. The model uses only geometric relationships—so that imbalance ID results, dynamic modeling, etc. are not needed. This is very important for simplicity and robustness.

$$\hat{F}_{net} = \left((G^T G)^{-1} G^T \right) (T^{-1} (S - B))$$

$$S - B = I_i T G F_{net} + (E_{SFN} + E_{SSN})$$

$$I_i(i, i) = 0$$

$$I_i T$$

$$\hat{F}_{net_i} = \left((I_i T G)^T (I_i T G) \right)^{-1} (I_i T G)^T (S - B)$$

LS estimation is repeated once for each possible failure mode: (1) no failures, and then (2-9) once for each situation where a single strain gauge would have failed, reading zero plus noise.

an identity matrix with the (i,i) element set to zero

is not invertible, so the equation cannot be pre-multiplied

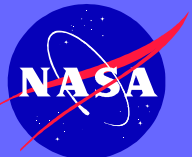
is calculated for each failure mode

Residual, $r_{i,k}$, from the least squares calculation is found as follows.

$$r_{i,k} = \left\| (S - B)_{measured,k} - (S - B)_{estimated, assuming i failed,k} \right\|$$

$$r_{i,k} = \left\| (S - B)_{measured,k} - I_i T G \hat{F}_{net_i,k} \right\|$$

$$r_{i,k} = \left\| (S - B)_{measured,k} - I_i T_k G \left((I_i T_k G)^T (I_i T_k G) \right)^{-1} (I_i T_k G)^T (S - B)_{measured,k} \right\|$$



Sensor FDIR steps

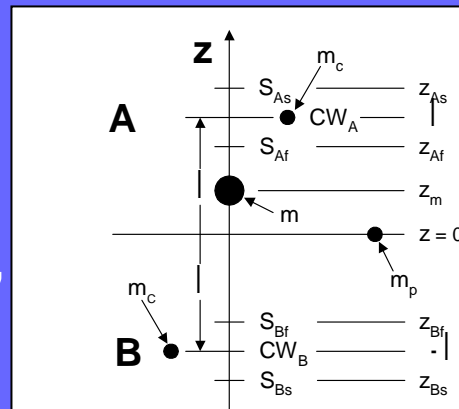
1. Sample spin angle encoder and estimate ψ . Use this to calculate T and T^{-1} .
2. Sample strain gauges and calculate the $(S-B)$ vector.
3. Calculate \hat{F}_{net} for the case of no SG failures present, indicated as \hat{F}_{net_0} .
4. Calculate \hat{F}_{net} for each SG failure case to be considered, indicated as $\hat{F}_{net_1} \cdots \hat{F}_{net_8}$.
5. Calculate the residuals associated with each potential fault mode, $r_{0,k} \cdots r_{8,k}$.
6. Compute the running modified likelihood function for each potential fault mode, $\sum r_0^2, \dots, \sum r_8^2$, as the sum over the most recent N samples (where N is tuned based on the desired rate of response in FDI vs. the noise level present).
7. Find the closest and second closest fault mode matches, $i_{closest}$ and $i_{second\ closest}$, corresponding to the lowest and second-to-lowest values of $\sum r_i^2$. Compute the generalized likelihood ratio as the ratio of these values, $\gamma = \frac{\sum r_{i_{closest}}^2}{\sum r_{i_{second\ closest}}^2}$.
8. If γ is below a specified threshold, and $i_{closest}$ is different than the presently isolated fault mode, $i_{isolated}$, declare $i_{closest}$ as the isolated fault mode (set $i_{isolated} = i_{closest}$). This step accomplishes the fault detection and isolation (FDI). Here, the detection and isolation are performed at the same step, which is not always the case.
9. Use $\hat{F}_{net_{isolated}}$ (already calculated in step 4, above) as \hat{F}_{net} in the remaining autobalancing calculations (e.g., use $\hat{F}_{net_{isolated}}$ where $\Gamma T^{-1}(S-\hat{B})$ is used). This step implements the reconfiguration (R), if needed.

Important aspects:

- Calculations used for FDI (i.e., the calculation of \hat{F}_{net_i}) can then be used directly in the reconfiguration (R). Reconfiguration involves simply using the \hat{F}_{net_i} value corresponding to the failure mode isolated, $\hat{F}_{net_{i_{closest}}}$, rather than the \hat{F}_{net} for the case of no failures, \hat{F}_{net_0} .
- Independent of the dynamical model and disturbance forces that may be acting on the rotor. It simply looks for self-consistency among the various redundant sensors that measure forces on the (assumed rigid) rotor. This approach can be applied directly to the ISS Centrifuge design, even though that has a compliant suspension and uses displacement sensors instead of force sensors.

Imbalance parameter estimation

- Use net force/torque vector from previous step
- Subtract effect of CWs, since known exactly
- Fit estimated force/torque data to dynamical model incorporating: dynamical model incorporating: gravity, centrifugal force, rotor angular accel, coriolis due to moving imbalance, imbalance acceleration. All for point mass and mass couple imbalance models.
- Estimate (choice): imbalance pos, vel, acc, sensor bias, spin axis alignment
- Details in paper.



A (B) refers to the upper (lower) part of the disk
 m_p , m_c are the imbalance masses
 m is the mass of the disk

CW_A , CW_B are the planes of the counterweights ($z = \pm l$ by definition)

S_{As} is the plane of the upper (A) spinning (s) strain gauges (S)
 S_{Af} is the plane of the upper (A) fixed (f) strain gauges (S)
 S_{Bs} is the plane of the lower (B) spinning (s) strain gauges (S)
 S_{Bf} is the plane of the lower (B) fixed (f) strain gauges (S)
 z_m is the z-axis coordinate of the disk c.o.g.

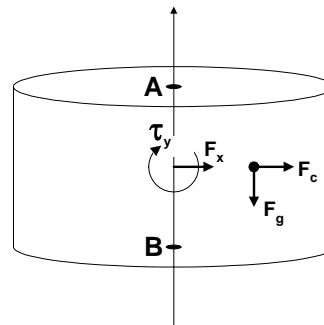
Z_{As} is the z-coordinate of S_{As}

Z_{Af} is the z-coordinate of S_{Af}

Z_{Bs} is the z-coordinate of S_{Bs}

Z_{Bf} is the z-coordinate of S_{Bf}

$z = 0$ is chosen arbitrarily as the midpoint between CW_A and CW_B



F_a is the force on the point masses due to angular acceleration (not shown in the figures)

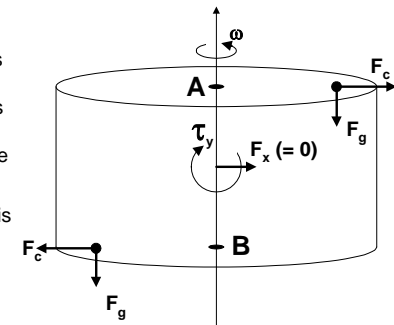
F_c is the force on the point masses due to centrifugal acceleration

F_g is the force on the point masses due to gravity

F_x is the net force on the disk in the +x direction (F_y is not shown)

τ_y is the net torque about the y axis of the disk (τ_x is not shown)

Forces due to imbalance motion (coriolis and acceleration) are not shown here.



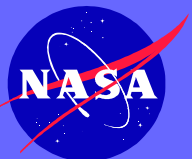
Counterweight control and FDIR

- Map estimated imbalance state to CW locations to null it.
- Physical redundancy accounted for, used in reconfiguration.
- CW control (e.g., allocation of redundancy, controller bandwidth, etc.) completely independent of imbalance ID.
- Trivial to update autobalancing controller if CW configuration changes.
- FDI presently assumes existence of CW encoders. More difficult, but possible without.
- SG and CW fault tolerance would allow uninterrupted operation—important to science planning, may be important for safety.

$$\begin{bmatrix} \delta_1 \\ \delta_2 \\ \delta_3 \\ \delta_4 \end{bmatrix} = \frac{-1}{2m_{CW}} \begin{bmatrix} m_p \hat{x}_p + 2m_c \hat{x}_c \\ m_p \hat{y}_p + 2m_c \hat{y}_c \\ m_p \hat{x}_p - 2m_c \hat{x}_c \\ m_p \hat{y}_p - 2m_c \hat{y}_c \end{bmatrix}$$

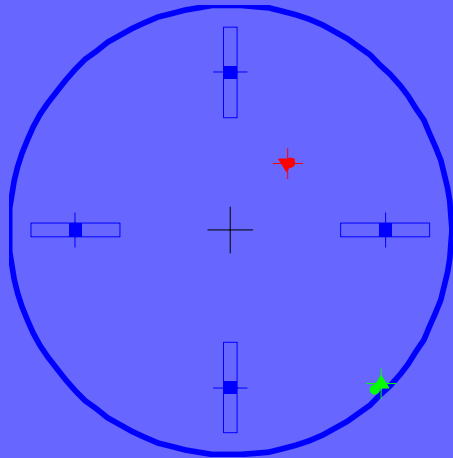
$$\begin{bmatrix} \delta_{1A} \\ \delta_{2A} \\ \delta_{1B} \\ \delta_{2B} \\ \delta_{3A} \\ \delta_{3B} \\ \delta_{4A} \\ \delta_{4B} \end{bmatrix} = \frac{1}{2} \begin{bmatrix} 0 & 0 & 0 & 0 \\ 0 & 1 & 0 & 0 \\ 2 & 0 & 0 & 0 \\ 0 & 1 & 0 & 0 \\ 0 & 0 & 1 & 0 \\ 0 & 0 & 0 & 1 \\ 0 & 0 & 1 & 0 \\ 0 & 0 & 0 & 1 \end{bmatrix} \begin{bmatrix} \delta_1 \\ \delta_2 \\ \delta_3 \\ \delta_4 \end{bmatrix} + \begin{bmatrix} \delta_{1A}^{frozen} \\ 0 \\ -\delta_{1A}^{frozen} \\ 0 \\ 0 \\ 0 \\ 0 \\ 0 \end{bmatrix}$$

$$\begin{bmatrix} \delta_{1A} \\ \delta_{2A} \\ \delta_{1B} \\ \delta_{2B} \\ \delta_{3A} \\ \delta_{3B} \\ \delta_{4A} \\ \delta_{4B} \end{bmatrix} = \frac{-1}{4m_{CW}} \begin{bmatrix} 0 & 0 & 0 & 0 \\ 0 & 1 & 0 & 0 \\ 2 & 0 & 0 & 0 \\ 0 & 1 & 0 & 0 \\ 0 & 0 & 1 & 0 \\ 0 & 0 & 0 & 1 \\ 0 & 0 & 1 & 0 \\ 0 & 0 & 0 & 1 \end{bmatrix} \begin{bmatrix} m_p \hat{x}_p + 2m_c \hat{x}_c \\ m_p \hat{y}_p + 2m_c \hat{y}_c \\ m_p \hat{x}_p - 2m_c \hat{x}_c \\ m_p \hat{y}_p - 2m_c \hat{y}_c \end{bmatrix} + \begin{bmatrix} \delta_{1A}^{frozen} \\ 0 \\ -\delta_{1A}^{frozen} \\ 0 \\ 0 \\ 0 \\ 0 \\ 0 \end{bmatrix}$$

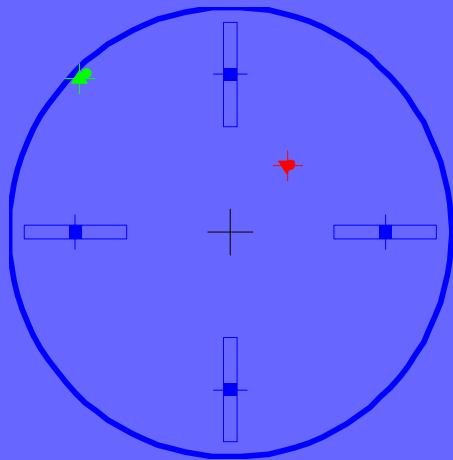


MATLAB simulation/animation

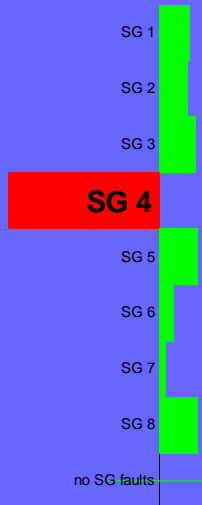
upper plane - imbalance, counterweights



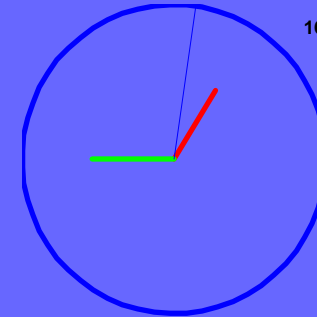
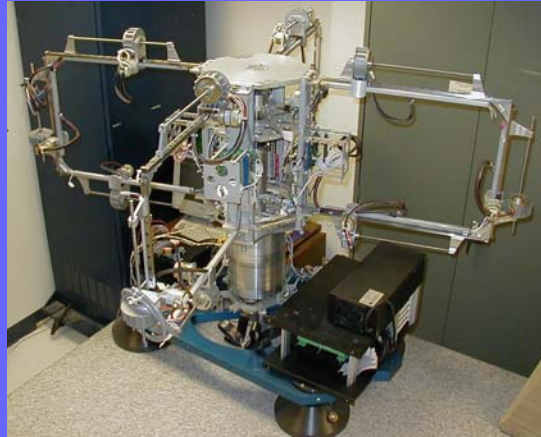
lower plane - imbalance, counterweights



sensor FDI



- + actual point-mass imbalance
- + actual mass-couple imbalance
- ID'ed point-mass imbalance
- ID'ed mass-couple imbalance
- ▼ residual point-mass imbalance
- ▲ residual mass-couple imbalance
- counterweights



16

- upper force
- lower force
- rotor angle

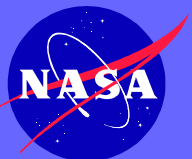
rotor speed = 0.454 rps
artificial gravity = 0.995 g

Blue line indicates zero-degree angle of the rotor. Red and green vectors indicate measured bearing forces, including sensor noise, vibrations, and imbalances, in the upper and lower planes. Since SG #4 has failed, the green vector has very little y-component (only noise). The scale factor (16) indicates that the radius of the blue circle is 16 Newtons, very large because the counterweight motion has been disabled in this simulation.

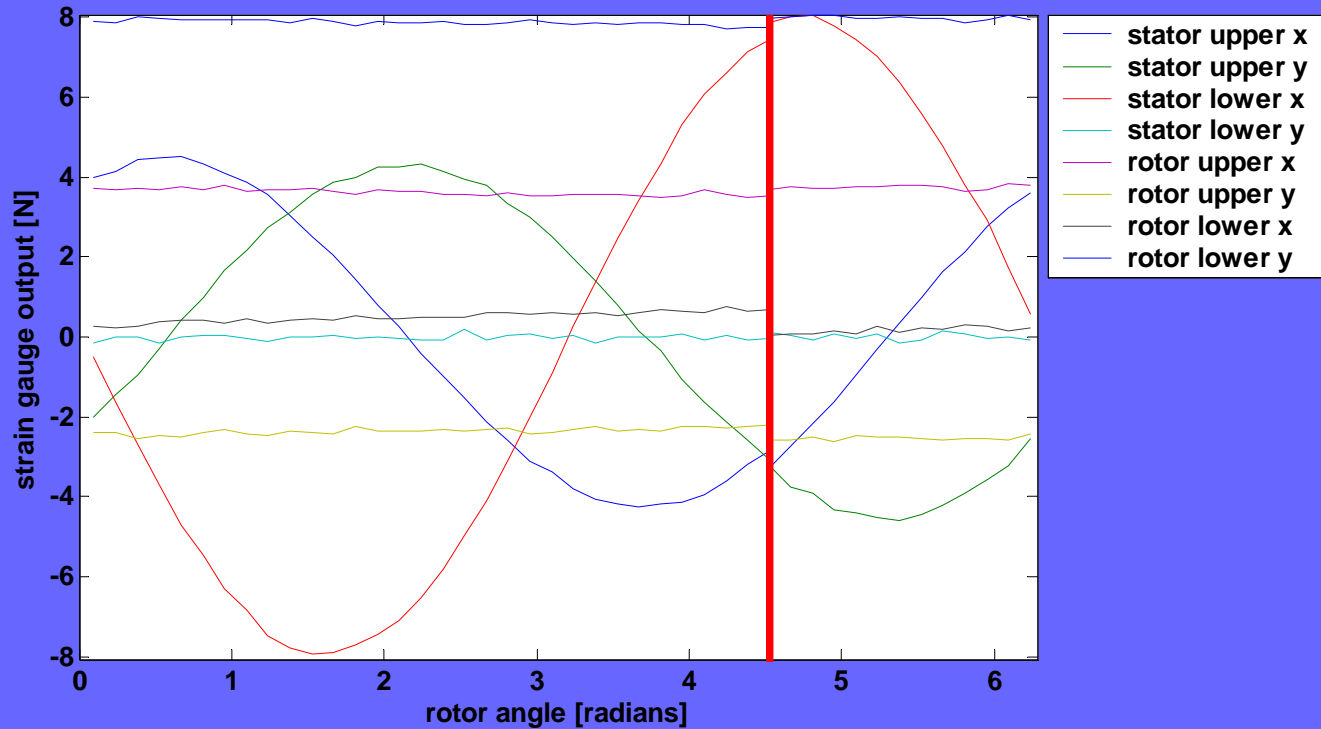
Control panel is used to control the simulation, starting/stopping the rotor spin, counterweights, and simulated random imbalance motion. Sensor and counterweight failures are also controlled. The imbalance may be "driven" manually (rather than the pseudo-random walk) by using the mouse to drag the blue circle joystick emulator on the right.

Joystick controls ...		Stop rotor	
[xp, yp(0)/xc, yc(1)]	8 7	[spinning(0)/stopped(1)]	
Imbalance motion		Imbalance state	
[stopped(0)/moving(1)]	6 5	[OK(0)/excessive(1)]	
CW motion		Sensor failure	
[disabled(0)/enabled(1)]	4 3	[none(0)/single(1)]	
CW Failure		ID speed	
[none(0)/single(1)]	2 1	[slow(0)/fast(1)]	
Noise x	Spin rate		
[0.0-1.0]	[0.0-0.68 rps]		

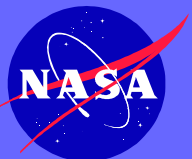
State of imbalance, imbalance-identification, and imbalance-cancellation are shown for upper and lower CW planes. Results of the SG FDI indicate that SG #4 has failed. Automatic reconfiguration following the fault isolation enables the identification to remain very accurate, as shown.



SG outputs, with SG fault



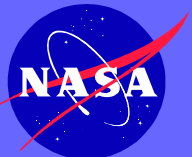
8 strain gauge signals are shown, plotted against the rotor angle. The vertical red line shows the beginning/end of the most recent revolution. If the imbalance were not moving, there were no vibration or sensor noise, and no failures were present, the 4 rotating gauges would read constant values and the 4 fixed gauges would have sinusoidal values (2 pairs 90 degrees in phase apart). However, "stator lower y" has failed, resulting in a reading of zero + noise.



Extension to ISS Centrifuge

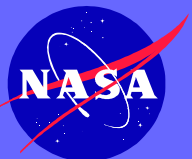
Key novel concepts in the present design will apply directly to ISS design:

- Modeling the rotor as a rigid body, and condensing all sensor measurements at each time update to a concise representation of the imbalance-induced forces and moments on the rotor.
- A control system that follows an indirect adaptive control architecture. It explicitly estimates the imbalance parameters, with the effect of counterweights calculated and subtracted out. Then a straightforward counterweight control system drives the CWs to null the total imbalance.
- Sensor FDIR ties in directly with the estimation of imbalance forces and moments, allowing efficient FDI, and then R by ignoring the failed sensor.
- Actuator FDIR ties in directly with the CW control system, allowing hardware redundancy to account for a stuck CW.
- Combined sensor and actuator FDIR systems should allow autonomous fault tolerance, allowing the system to continue operation in the face of sensor or actuator faults. The segmentation of sensing/identification and actuation/balancing facilitates this reconfiguration, as, for example, a failed actuator does not impact the identification at all.



Conclusion

- Algorithms that provide automatic balancing and autonomous fault tolerance for a space-based centrifuge have been derived and successfully implemented in software simulation. Although developed for an Earth-based simulator, the underlying principles may be extended for application to the ISS Centrifuge design which has a 5-axis vibration isolation mechanism suspension and displacement sensors.
- The architecture, which is similar to an indirect adaptive control architecture, allows careful and independent tuning of identification and control bandwidths, which is a key challenge for this application.
- The sensor FDIR method presented uses maximum likelihood theory and is integrated closely with the imbalance identification algorithms, facilitating reconfiguration in the case of a sensor fault. This method does not rely on the rotor dynamical model, and is independent of rotor disturbances, relying only on the self-consistency of the redundant sensor suite.
- The overall architecture and FDIR algorithms should be applicable to other aerospace systems that require automatic, fault tolerant, on-line identification and control of system properties.



Acknowledgments

- Funding for the research reported here, including development of the SSRL centrifuge prototype, was provided by NASA Headquarters Code R and the Space Station Biological Research Project (SSBRP) at NASA Ames Research Center.
- Thanks to other members of the NASA Ames SSRL who contributed to the centrifuge prototype development: Michael C. Guerrero, Alessandro Galvagni, and Ramin Esahagi.
- Thanks to NASA Ames Centrifuge Office personnel for support and interesting discussions related to Centrifuge Rotor control: Robert D. Barber, Dr. Jeremy H. Yung, Dr. Andrew S. Elliott, Martin D. Hasha, Roy Hampton, Dr. Ann L. Blackwell, Daniel L. Dittman, Li S. Chang, Dr. Jack M. Peng, and Epifanio Munoz.
- Thanks to the many members of the JAXA/Toshiba/NEC Toshiba Space Systems team for the open technical discussions of the various Centrifuge Rotor controller designs: Dr. Koichi Ohtomi, Osamu Nishimura, Ryo Furukawa, Hiroyuki Katayama, Takuya Kanzawa, Yoshitaka Ooi, and Osamu Kawamoto.

